ENVIRONMENTAL Science & Technology

ARTICLE

pubs.acs.org/est

CO_2 Modeling in a Deep Saline Aquifer: A Predictive Uncertainty Analysis Using Design of Experiment

Baozhong Liu and Ye Zhang*

Department of Geology and Geophysics, University of Wyoming, Laramie, Wyoming 82071, United States

Supporting Information

ABSTRACT:

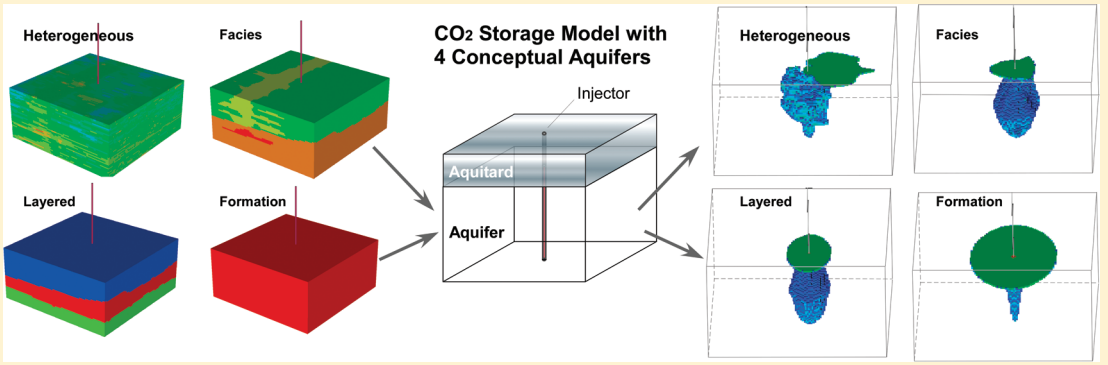

When field data are limited, stratigraphic models are used instead of detailed, fully heterogeneous models (FHM) to represent deep saline aquifers in numerical simulations of CO_2 storage. This study evaluates parameter sensitivity and prediction uncertainty of three stratigraphic models of decreasing complexity (i.e., facies, layered, formation) against that of a FHM. For select simulation outcomes (i.e., CO_2 mass profiles, gas plume shape, brine leakage), parameter sensitivity and associated prediction uncertainty are compared among the models, with the FHM serving as a reference. The analysis is conducted using the computationally efficient design of experiment (DoE) and response surface (RS) methodology. Results suggest that when a competent caprock exists (permeability $<1 \times 10^{-4}$ mD), the facies and layered models are capable of capturing the most important sensitivity parameters of the FHM, that is, residual gas saturation, heterogeneity variance, and salinity. Using the important parameters identified by DoE, RS modeling then suggests that the same two models also capture the ranges of predictions in mobile gas, trapped gas, and brine leakage. The formation model is less accurate in capturing the sensitivity and prediction ranges of the FHM, although it is accurate in predicting brine leakage into the overlying formation.

1. INTRODUCTION

Carbon dioxide (CO_2) capture and storage (CCS) into deep saline aquifers is considered a promising option to mitigate global climate change.[1] To assess a storage formation, reservoir simulation is commonly performed using a site geologic model. Due to technical or economical reasons, data needed to build a detailed site model are often lacking. As a compromise, stratigraphic models are built in which facies or depositional zones, or even the entire aquifer, are assumed homogeneous. Since natural aquifers exhibit intrinsic permeability (k) heterogeneity at multiple scales, stratigraphic models are conceptual simplifications created based on the level of data support. It is important to understand not only the adequacy of such models in representing natural systems, but also if an optimal complexity of the stratigraphic model exists that can lead to a cost-effective strategy in data collection and reservoir modeling. However, a key difficulty exists here: in addition to uncertainty in aquifer permeability, uncertainty in multiple geologic and engineering variables exists. Determination of an optimal stratigraphic model must be evaluated within a full parameter space, which is computationally challenging if CO_2 storage is modeled at the field (or larger) scales using traditional simulation techniques.[2]

In this study, a design of experiment (DoE) and response surface (RS) methodology is used to conduct a parameter sensitivity study and prediction uncertainty analysis. The methodology is computationally efficient, suitable for the uncertainty analysis of data-poor settings.[3,4] To eliminate uncertainty in k pattern and focus only on parameter uncertainty, a 3D synthetic aquifer is created to represent a groundtruth model with a fully known permeability pattern. This fully heterogeneous model (FHM) is used to gauge the performance of three stratigraphic models of decreasing complexities: a facies model with eight units, a layered model with three units, and a formation model with one unit

Received: September 18, 2010
Accepted: March 16, 2011
Revised: March 10, 2011

   dx.doi.org/10.1021/es103187b | Environ. Sci. Technol. XXXX, XXX, 000–000

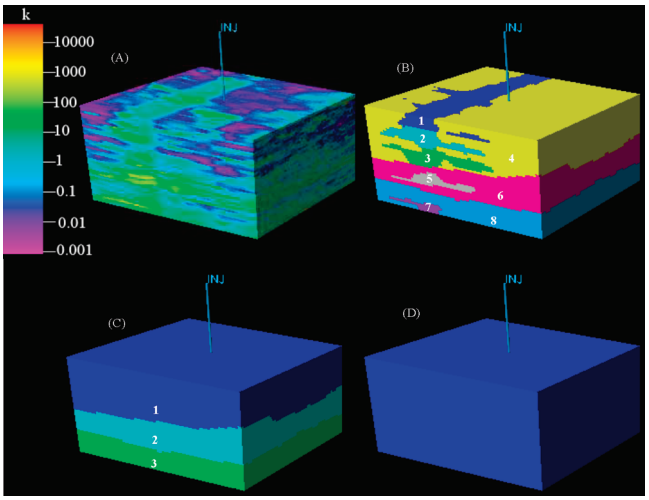

Figure 1. Aquifer models of this study: (A) fully heterogeneous model (permeability is shown in mD when the system lnk variance is 7.0); (B) facies model with 8 units (unit ID is shown); (C) layered model with 3 units; (D) formation model with 1 unit. All models employ a uniform grid, with 101 × 101 × 41 block cells. To all models, a homogeneous caprock is added (not shown).

(Figure 1). Since aquifers can exhibit different degrees of permeability heterogeneity and preferential CO_2 channeling can occur in highly heterogeneous systems,[5] the FHM is scaled to increasing natural log permeability (lnk) variances. Variance of lnk is a key uncertainty parameter analyzed. At each variance level, the stratigraphic models are upscaled from the FHM (detail is described elsewhere[6]).

For our set of models (i.e., stratigraphic models are conceptual equivalents of the FHM), multiple uncertain input parameters are defined, their selection based on typical uncertainty variables and their ranges encountered at CCS sites. For a suite of prediction outcomes, a stratigraphic model is considered optimal if it can capture both parameter sensitivity and prediction uncertainty of the FHM. Specifically, within the full parameter space, the stratigraphic models are examined in three aspects: (1) accuracy in predicting CO_2 mass profiles, plume shape, and brine leakage; (2) ability to capture the most important parameters impacting the outcomes of the FHM; (3) ability to capture the prediction envelopes of the FHM.

Worldwide saline aquifers suitable for CCS can be found at a variety of depths. To explore the effect of depth on model sensitivity and prediction uncertainty, the models are placed at 1, 2, and 3 km, respectively. The upper limit of 1 km is slightly deeper than the typical depth threshold where CO_2 is considered supercritical (~800 m). Since geothermal gradient is one of the parameters varied, this depth ensures that CO_2 remains supercritical in the model. The lower limit is selected based on a cost threshold:[7] below 3 km, storage efficiency generally decreases and cost per ton of injection increases. The uncertainty analysis is repeated at each depth.

In the following sections, the uncertainty analysis is introduced, followed by results, discussions, and conclusions. Supporting Information (SI) is attached, including details of CO_2 simulation, parameters varied in the sensitivity analysis (SA), and gas prediction outcomes.

2. MATERIALS AND METHODS

2.1. Model Creation. Using images of sediment created in a laboratory flume, a FHM is created (Figure 1A). The model is 2525 m long, 2525 m wide, and 102.5 m thick, as a host formation of ~1 km^2 by 100 m is required to store CO_2 from a single power plant.[8] Using facies analysis, a stratigraphic model is created containing eight facies units (Figure 1B). Since the flume deposit emulates a fluvial system with multiple depositional episodes, a 3-Unit layered model is created (Figure 1C). Each layer consists of several units of the facies model (e.g., layer 1 corresponds to facies units 1−4, etc). A formation model is also created (Figure 1D). The 8-, 3-, and 1-Unit models are hosted within a sedimentary hierarchy, representing conceptual models developed at decreasing complexity (i.e., heterogeneity resolution) from the FHM. To ensure that models are comparable, equivalent permeability is computed for each unit of stratigraphic models using an upscaling technique.[6] Under the same fluid driving forces, all models predict similar flow rates.[6] Since CO_2 storage and leakage are both of interest, a 40 m thick (10 vertical cells) caprock is placed above the aquifer. The caprock is assumed to be homogeneous. The combined aquifer and caprock is referred to as a storage model. All models employ the same grid, with 520 251 block cells.

2.2. CO_2 Simulation. CO_2 is injected using a single vertical well at the model center, perforated in the aquifer only. In the SA, the total injected CO_2 is fixed (538 063 t), whereas the injection rate is varied as an uncertain input variable (0.45−0.90 kg/s). Thus, injection duration varies from 20−40 years, corresponding to the changing injection rate. A 500-year postinjection monitoring period is simulated. All models are given a laterally open boundary. An external aquifer is placed above the caprock to provide a receptacle to receive CO_2 and brine that has leaked through the caprock (details of the simulations can be found in the SI).

To simplify the simulation and sensitivity analysis, this study employs several assumptions. First, fluid rock reactions are not considered, which can be assumed negligible for an aquifer with quartz-dominated mineralogy.[1] Nonisothermal effects are ignored, as are drying-out, salting-out, and coupled flow and geomechanical feedbacks. Viscous fingering due to CO_2 dissolution in brine, which typically requires a cm-scale grid size, is not modeled. Capillary pressure (Pc) is assumed negligible, thus a single fluid pressure is computed. In field-scale modeling, Pc can be neglected when there exist strong viscous or gravity forces.[2] However, we acknowledge the potentially important role capillary entry pressure plays in deterring CO_2 breakthrough into the caprock. This effect will be considered in future work.

2.3. Sensitivity Analysis and Response Surface Modeling. Sensitivity analysis (SA) for each model is conducted using DoE.[9] Unlike the conventional analysis whereby parameters are varied one at a time while keeping all others fixed, DoE varies subsets of the parameters simultaneously according to a design table. Results are compiled and examined with multivariate analysis of variance (MANOVA) to identify parameters that have statistically significant effects on a prediction outcome. Though a variety of designs are available (same design can be used for multiple outcomes), a two-level Plackett-Burman (PB) design is used which is the most effective when parameters varied in the SA (or factors) are orthogonal, that is, uncorrelated. Compared to other designs (e.g., fractional factorial), the PB design is parsimonious in selecting a parameter subset for simulations, providing large savings in program execution time when the problem size is large and the physics to be solved complex. However, the PB design can only identify main effects as well as any confound interactions with the main effects. It is the most useful as a screening tool that can quickly identify significant uncertainty factors. In reservoir

dx.doi.org/10.1021/es103187b |Environ. Sci. Technol. XXXX, XXX, 000–000

Table 1. Input Parameters and Their Ranges Varied in the SA for the FHM. −1, 0, +1, Indicate Low, Mid, And High Values Assigned to Each Parameter, Respectively. All Parameters Are Independent of One Another

	AquG (m/m)	TG (°C/m)	VAR	SGR	SAL ppm	q kg/s	krock mD
−1	−0.03	0.025	0.1	0.06	10 000	0.45	10^{-8}
0	0.00	0.040	1.0	0.30	135 000	0.68	10^{-6}
1	0.03	0.050	7.0	0.42	260 000	0.90	10^{-4}

simulation, PB is used in scoping studies to guide early data collection.[10]

The RS method consists of fitting a polynomial function to each outcome of the DoE analysis.[11] The function is based on the factors previously identified as important to the outcome. Prior to RS modeling, three values for each factor are necessary in the DoE analysis, that is, −/0/+ values. Such values can correspond to key probabilities of a factor, but it is not a requirement. The RS model is considered a predictive model of the relationship between input factors and simulation outcomes (responses). Using RS, a range of predictions can be made by varying these factors within their respective ranges. The factor values can be continuous, as opposed to (discrete) end-point and midpoint values specified in the design. Since prediction using RS is fast, it is used in reservoir analysis as a proxy model to analyze prediction uncertainty.[3] For example, if a minimum or maximum response exists within the factor region, this can be identified from the RS model using optimization techniques. Monte Carlo analysis can also be run on the RS (by randomly drawing factors), leading to a probability density function of the outcome. Such analyses are orders of magnitude faster than one using reservoir simulations. In this study, the DoE and RS analysis is performed with JMP 8.0, a package developed by Statistical Analysis Software, Inc.

2.3.1. Input Parameters. A SA is conducted for all models using DoE. For each model, seven input parameters are varied: (1) vertical gradient of background aquifer flow (AquG), (2) geothermal gradient (TG), (3) level of aquifer heterogeneity (i.e., variance of lnk, VAR), (4) maximum residual gas saturation (SGR), (5) salinity of formation water (SAL), (6) injection rate (q), and (7) caprock permeability (krock). The parameters and their ranges are summarized for the FHM in Table 1. For the stratigraphic models, the same parameters are varied, though VAR now represents the variance of the FHM (aquifer zone only), from which units of the stratigraphic models are homogenized. Justification for choosing the parameters and their ranges is provided in the SI.

2.3.2. Model Outcomes. Five outcomes are evaluated for CO_2 modeling: (1) mobile gas-phase CO_2 (mobile gas), (2) trapped gas-phase CO_2 (trapped gas), (3) dissolved aqueous-phase CO_2 (dissolved gas), (4) brine displaced from the storage model into the overlying aquifer, and (5) gas-phase leakage into the same aquifer. Since CO_2 modeling contains two periods (injection and monitoring) and during each period, viscous force, gravity, and heterogeneity can exert different influence on flow, sensitivity of model outcomes to parameters is expected to change with time. Each outcome is exported at six different times: at the end of injection and at 100, 200, 300, 400, and 500 years postinjection.

2.3.3. DoE and RS Modeling. For the seven factors varied in the SA, a PB design table is shown (Table 2). A center run is added where all factors assuming their median ("0") values. This run is optional for identifying important factors, but is necessary for identifying parameter nonlinearity and providing center-valued responses for RS modeling. After simulating all runs in Table 2, model outcomes at the select output times are compiled. For each outcome (at each time), parameter importance is determined by its main effect on the outcome at a specified statistical confidence level. Using MANOVA, a list of the most important to the least important parameters can be identified. The FHM follows this design exactly. For the stratigraphic models, VAR is not a direct input factor. Instead, the level of VAR determines a set of equivalent permeabilities that has been computed by homogenizing the FHM.[6] For all models, at all depths (1, 2, and 3 km), 4 × 13 × 3 = 156 simulations are conducted.

Table 2. PB Design with Seven Factors. An Optional Central Run (Run 7) Is Added. Corresponding Parameter Values for −1/0/1 Are Shown in Table 1

run	AquG (m/m)	TG (°C/m)	VAR	SGR	SAL (ppm)	q (kg/s)	krock (mD)
1	−1	−1	−1	1	−1	−1	1
2	−1	−1	1	−1	−1	1	−1
3	−1	−1	1	−1	1	1	1
4	−1	1	−1	−1	1	−1	1
5	−1	1	−1	1	1	1	−1
6	−1	1	1	1	−1	−1	−1
7	0	0	0	0	0	0	0
8	1	−1	−1	−1	1	−1	−1
9	1	−1	−1	1	−1	1	1
10	1	−1	1	1	1	−1	−1
11	1	1	−1	−1	−1	1	−1
12	1	1	1	−1	−1	−1	1
13	1	1	1	1	1	1	1

Prediction uncertainty of all models is evaluated following these steps: (1) RS models are first developed for the FHM for multiple outcomes, and at multiple times. These models are verified against the simulation results; (2) for the same outcomes, RS models are developed and verified for the stratigraphic models. (3) using RSs, at each output time, minimum and maximum responses of an outcome are generated. A time-dependent prediction envelope is created. (4) for the same outcome, prediction envelopes are compared among the models. (5) above analysis is repeated at different depths, following a DoE analysis conducted using CO_2 simulation results at that depth.

3. RESULTS AND DISCUSSION

Results of this study follow five themes: (1) DoE results of the FHM are analyzed first, providing insights into parameter sensitivity for a model with fully resolved permeability. (2) DoE results of all models are compared to evaluate parameter sensitivity in response to changing conceptual models (Table 3). For select simulation runs, gas profiles, plume shape, and CO_2/brine leakage are compared. (3) RS results of all models are compared to identify an appropriate stratigraphic model that can capture the prediction envelopes of the FHM. (4) All results above pertain to a system depth of 2 km—the center value of depth. The analysis is repeated at 1 and 3 km depths to evaluate its effect on parameter sensitivity and prediction uncertainty. (5) Time scale of simulation is reduced to emulate pilot-scale scenarios. For most runs, gas-phase leakage through the caprock

Table 3. Results of SA at 2 km Depth. Parameters Important to an Outcome Are Listed from the Most Important to the Least Important at a 90% Confidence Level. "Brine Leakage" Is Brine That Has Leaked through the Caprock into the Overlying Aquifer

outcomes	models	end of injection	monitoring period (years after injection ends)				
			100	200	300	400	500
trapped gas	FHM	SGR/VAR/SAL	SGR/VAR/SAL	SGR/VAR/SAL	SGR/SAL/VAR	SGR/SAL/VAR	SGR/SAL/VAR
	8-UNIT	SGR	SGR/VAR/SAL	SGR/VAR/SAL	SGR/VAR/SAL	SGR/VAR/SAL	SGR/VAR/SAL
	3-UNIT	SGR/VAR	SGR/VAR/SAL	SGR/VAR/SAL	SGR/VAR/SAL	SGR/VAR/SAL	SGR/VAR/SAL
	1-UNIT	SAL/SGR/q/TG	SGR/SAL	SGR/SAL	SGR/SAL	SGR/SAL	SGR/SAL
dissolved gas	FHM	SAL/VAR/TG	SAL/VAR/SGR	SAL/VAR/SGR	SAL/VAR/SGR	SAL/VAR/SGR	SAL/VAR/SGR
	8-UNIT	SAL/TG/VAR/q	SAL/VAR	SAL/VAR	SAL/VAR/TG/SGR	SAL/VAR/SGR/TG	SAL/VAR/SGR/TG
	3-UNIT	SAL/TG/VAR/q	SAL/VAR/TG	SAL/VAR/TG/SGR	SAL/VAR/TG/SGR	SAL/VAR/TG/SGR	SAL/VAR/TG/SGR
	1-UNIT	SAL	SAL/TG/SGR	SAL/TG/SGR	SAL/SGR/TG	SAL/SGR/TG/VAR	SAL/SGR/TG
mobile gas	FHM	VAR	SGR/VAR	SGR/VAR	SGR/VAR	SGR/VAR	SGR/VAR
	8-UNIT	VAR/SAL	SGR/VAR/TG/AquG/SAL/q	SGR/VAR/TG/SAL/AquG	SGR/VAR/SAL	SGR/VAR	SGR/VAR/SAL
	3-UNIT	SAL/VAR/SGR	SGR/VAR/TG/AquG/SAL	SGR/VAR/TG/AquG	SGR/VAR/TG	SGR/VAR	SGR/VAR
	1-UNIT	SAL/SGR/q	SGR/VAR	SGR/VAR	SGR/VAR	SGR/VAR	SGR
brine leakage	FHM	krock	krock/AquG	krock/AquG	krock/AquG	krock/AquG	krock/AquG
	8-UNIT	krock	krock/AquG	krock/AquG	krock/AquG	krock/AquG	krock/AquG
	3-UNIT	krock	krock/AquG	krock/AquG	krock/AquG	krock/AquG	krock/AquG
	1-UNIT	krock	krock/AquG	krock/AquG	krock/AquG	krock/AquG	krock/AquG

is negligible, thus statistical tests on parameter importance to this outcome cannot be conducted.

3.1. Parameter Sensitivity of the FHM. For outcomes of the FHM, statistically important factors are identified at the 90% confidence level (Table 3). In predicting trapped gas, SGR, VAR, and SAL are the 3 most important factors over the entire simulation time. Their main effects are positive, indicating that increasing the value of each will lead to more residual gas trapping.

During monitoring, higher SGR leads to more trapping, as expected, since gravity override is significant, resulting in upward plume migration. At the trailing plume, gas saturation (S_g) decreases (water imbibes), leading to residual trapping. During injection, however, SGR is also identified as important, suggesting that S_g is locally decreasing. This is confirmed by inspecting S_g over time. This could be due to a combination of gravity flow, dissolution, and injector pressure response to boundary condition. For example, when VAR = 7.0, gas plume sought out a high-k pathway in the aquifer and rose toward the caprock. At the end of injection, a small pool appeared beneath the caprock, and along the pathway, S_g can decrease locally when gravity outcompetes viscous drive. The injector pressure is also inspected: after reaching an initially higher value, pressure pulse reaches the boundary, injector pressure is adjusted slightly downward, which may cause S_g to decrease. Though the magnitude of this trapping is small, the amount trapped is controlled by SGR.

Increasing VAR results in more trapped gas: higher VAR leads to more lateral plume spreading, more brine contacts the gas, thus more trapping during imbibition. VAR shifts from being the second most important factor during the first 200 years, to being the third most important at longer time scales. VAR is important during injection and early monitoring, when gas flow and trapping is most active and thus more sensitive to heterogeneity. In later times, more mobile gas has migrated to the top of the aquifer, sampling less heterogeneity as the plume rises. Simultaneously, much of the gas in the lower aquifer becomes immobilized, thus heterogeneity of the exerts little impact on trapping there.

In predicting trapped gas, increasing SAL inhibits dissolution, leading to more gas available for migration, thus increased amount of residual gas trapping. However, due to less dissolution, the overall trapping (dissolved plus residual) may decrease.

In predicting dissolved gas, SAL is the most important factor exerting a negative effect over all times, as expected. VAR is the next most important, though its effect is positive. Larger VAR contributes to more lateral plume spreading, more brine is contacted by gas, and thus more dissolution.

In predicting mobile gas, VAR is the only important factor during injection; after injection, SGR is more important, followed by VAR. Both factors exert negative effects: when VAR is high, gas plume is dispersed, thus contacting more brine, resulting in enhanced residual trapping and dissolution. This leads to less mobile gas. When SGR is high, more gas is trapped, and thus less mobile gas. SGR is not important during injection, probably because imbibition is mildly active then, while VAR affects both trapping and dissolution. To quickly immobilize the plume in the aquifer, high variance and high residual gas saturation appear ideal.

In predicting gas-phase leakage, DoE analysis cannot be conducted since gas leakage through caprock is zero in most runs. Within the parameter space, the high krock (10^{-4} mD) is competent in deterring gas migration. The largest CO_2 leakage occurs in Run 4. The amount of the gas leaked is extremely small, but it is of interest to examine the causes. Run 4 has the most favorable combination of all parameters that contribute to leakage: an upward aquifer flow, high TG (more buoyant gas), low VAR (less lateral spreading, more upward migration), small SGR (less trapping, more mobile gas for migration), high SAL (less dissolution leading to more gas thus more mobile gas), low q (reduced viscous driving force, less lateral spreading), and high krock.

In predicting brine leakage, krock is the most important factor at all times, while AquG is additionally important during monitoring.

dx.doi.org/10.1021/es103187b |Environ. Sci. Technol. XXXX, XXX, 000–000

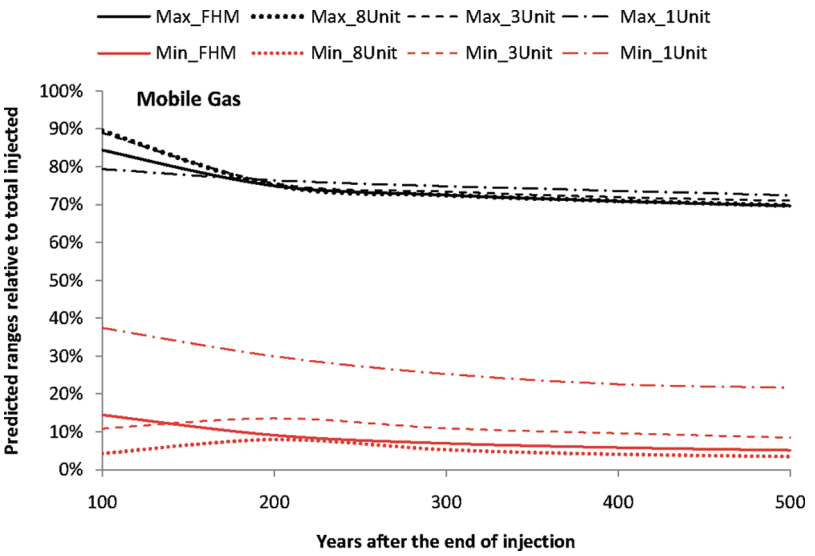

Figure 2. Prediction envelopes of the mobile gas predicted by all models. The amount of mobile gas is expressed in terms of percentage of the total injected gas.

Brine leakage is driven by pressure buildup in the aquifer, reflected by a higher rate during injection but lower rate during monitoring. After injection ceases, pressure at the injector dissipates. The strength and direction of the background flow become important. Thus, if short-term leakage is of concern, caprock permeability must be evaluated: a competent caprock for containing gas here is not competent in deterring brine migration. If long-term leakage is of interest, aquifer flow should be evaluated, though this form of leakage could be natural. Since CO_2 dissolves into brine, factors that contribute to brine leakage will also contribute to the leakage of dissolved CO_2 into the overlying formations.

3.2. Parameter Sensitivity of All Models. SA results of all models are compared (Table 3), with several observations: (1) in predicting brine leakage, sensitivity of the stratigraphic models is identical to that of the FHM. Due to k homogenization, these models predict similar fluid pressure as that of the FHM. Within the parameter space evaluated, formation model can be adequate in assessing brine leakage of a heterogeneous system. (2) when predicting trapped gas, SA results of the facies and layered models are close to those of the FHM. (3) when predicting dissolved gas, all stratigraphic models are sensitive to the same, most important, factor of the FHM (i.e., SAL), though they fail to consistently capture the secondary or tertiary factors. (4) when predicting mobile gas, SGR and VAR are the two most frequently occurring factors for all models.

Since VAR is consistently identified as an important parameter impacting gas predictions, three runs with low (Run 1), intermediate (Run 7), and high (Run 6) VAR are compared among the models, in terms of gas profile and plume shape predictions (see SI). Results suggest that, in gas predictions, both heterogeneity variance and heterogeneity resolution are important in controlling the accuracy of the stratigraphic models: when variance is fixed, higher resolution leads to greater accuracy; when resolution is fixed, higher variance leads to greater inaccuracy. However, brine leakage predicted by these models is almost identical, proving that accuracy in brine prediction is not affected by either heterogeneity variance or its resolution.

3.3. Response Surface Modeling. Within the parameter space, a prediction envelope can be created for each outcome using RSs. For each model, time-dependent prediction envelopes are created for the monitoring phase. The outcomes are: mobile gas (Figure 2), trapped gas (Figure 3), and brine leakage (Figure 4). The amount of dissolved gas depends on the other gas forms; its results are not presented. The envelopes are created by running a RS model to identify the minimum and maximum values of an outcome. However, when brine leakage is close to zero, extrapolation of RS predicts meaningless (negative) values. Only maximum leakage is determined. Results suggest that in predicting both mobile and trapped gas (thus dissolved gas), the facies and layered models are adequate for capturing the prediction envelopes of the FHM. The formation model suffers large errors in predicting minimum mobile gas and maximum trapped gas. Note that in comparing the prediction envelopes, factor combination that gives rise to a maximum mobile gas will likely correspond to a minimum trapped and dissolved gas, vice versa. In predicting maximum brine leakage, all models give nearly identical results, as expected.

Above results suggest that if an appropriate stratigraphic model is used, prediction envelopes generated using RSs of this model can potentially capture the prediction envelopes of the FHM generated with full-field simulations. This statement is approximately true, since prediction envelopes of the FHM were not generated using numerous reservoir simulations, but were instead generated by the RSs of the FHM. These RSs involve interpolation in the parameter space at unsampled parameter values. If the RS model is very accurate, minimum or maximum on the RS are expected to be similar to the true minimum or maximum. However, the PB design, though efficient (fewer runs), is of lower resolution. In the DoE and RS methodology, higher resolution schemes exist which use more simulations to gain greater accuracy in RS modeling. These designs will be evaluated in future work.

3.4. Effect of Depth. The above SA and RS results were examined at 2 km depth. The analysis is repeated at 1 and 3 km depths (see SI). Both parameter sensitivity and prediction uncertainty of the FHM and the ability of the stratigraphic models to capture them are similar to those identified at 2 km, suggesting that the above observations can be extended to other depths.

dx.doi.org/10.1021/es103187b |*Environ. Sci. Technol.* XXXX, XXX, 000–000

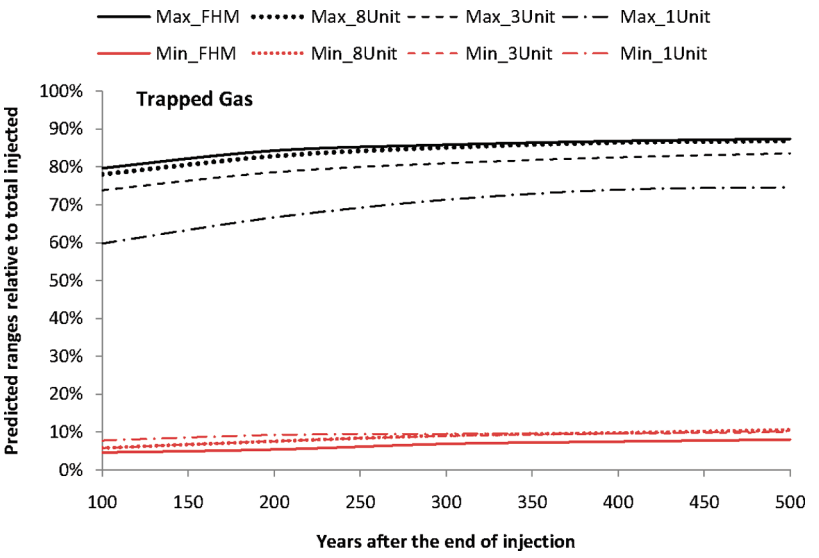

Figure 3. Prediction envelopes of the trapped gas predicted by all models.

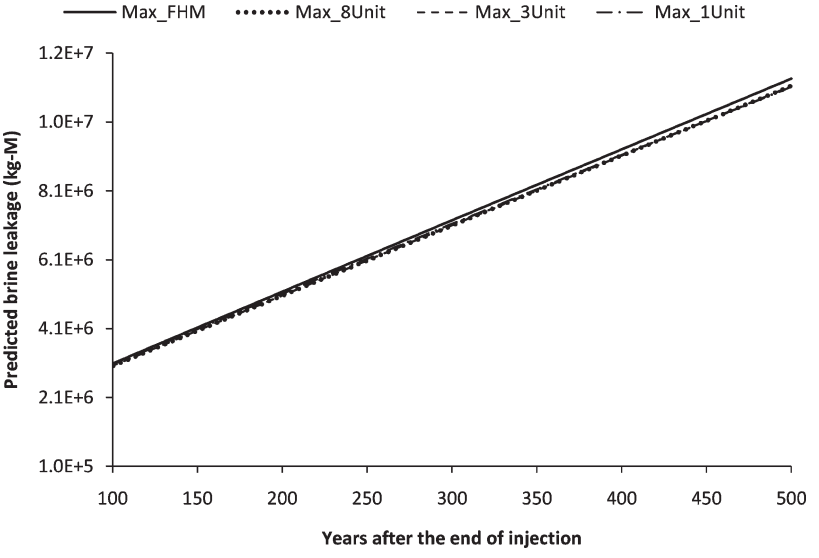

Figure 4. Maximum cumulative brine leakage predicted by all models.

3.5. Effect of the Amount of Gas Injected. Previous simulations use small, pilot-scale injection rates. To fill the storage model and evaluate the effect of k heterogeneity on predictions, a long simulation time is used. To make the model time scale comparable to those of pilot tests, SA is repeated at the 2 km depth with a shortened injection (2−4 months) and monitoring (2 years) duration. Injection rate is first doubled from previous ones to 0.9−1.8 kg/s, and then quadrupled (1.8−3.6 kg/s), though both are still within the range of pilot-scale tests.[12] Since the injection time is much shorter, even though the rate has increased, much less amount of gas is injected (1.6−3.3% of the previous amount). Comparing the new SA results with those of Table 3, new effects have risen in gas prediction: (1) at the end of injection, SAL becomes the most important factor impacting all gas forms and VAR has vanished. (2) postinjection, the most important factors remain identical with those of Table 3, though VAR has largely disappeared as an important factor influencing mobile and dissolved gas (its importance to trapped gas remains unchanged). For brine leakage, the sensitivity characteristics are nearly identical except TG and q become additionally important. Clearly, certain sensitivity is affected by the amount of gas injected in relation to reservoir pore volume. When this amount is small, much of the aquifer heterogeneity is not sampled, and VAR becomes less important to some predictions.

In summary, parameter sensitivity and prediction uncertainty of three stratigraphic models of decreasing complexity are evaluated against those of a FHM. Results suggest that, for the parameter space considered, facies and layered models are capable of capturing the most important sensitivity parameters of the FHM. The same two models also capture the ranges of predictions in mobile gas, trapped gas, dissolved gas, and brine leakage. The formation model is less accurate in capturing the sensitivity and prediction ranges of the FHM, but is accurate in predicting brine leakage. Thus, optimal model complexity should be selected based on the prediction metric of interest. In predicting gas flow and storage, the layered model appears optimal;

dx.doi.org/10.1021/es103187b |*Environ. Sci. Technol.* XXXX, XXX, 000–000

in predicting brine leakage (related to fluid pressure), the formation model appears optimal. Furthermore, for the models and parameters considered, permeability variance, gas relative permeability hysteresis, and salinity consistently impact one or more prediction outcomes, suggesting that they should be routinely evaluated in site assessments. In particular, when heterogeneity is of low variance, simple stratigraphic models can accurately predict plume shape and CO_2 mass fractions; when variance increases, models with higher heterogeneity resolution are needed. However, the importance of variance can diminish when the amount of gas injected is small. These observations are expected to be applicable to the full range of depths encountered in CCS operations.

Our results, however, are specific to the ranges of the parameters varied. For example, if an end-member value much greater than 10^{-4} mD is assigned to krock, its importance to predicting gas-phase leakage will likely change. At a typical storage site, information usually exists concerning caprock and its permeability. krock range here reflects a degree of prior knowledge. Since the DoE and RS methodology is applicable to field modeling, parameters and their ranges should be tailored to site-specific condition incorporating prior knowledge before uncertainty analysis is performed. Furthermore, results of this study are obtained using a screening design which sacrifices resolution for efficiency. Future work will investigate high resolution designs which can enhance the accuracy of RS modeling. Finally, a fixed aquifer geometry is evaluated with no dipping beds. Though variance of heterogeneity is varied for the FHM, its pattern is fixed. Future work will evaluate aquifers with different dip, geometry, and internal heterogeneity (e.g., weak versus strong connectivity in permeability). Capillary pressure effects will be modeled, as well as other potentially important variables and processes (e.g., vertical versus horizontal wells, lateral aquifer flow). Future work will also assess injection rates commensurate with those used in commercial-scale operations.

■ ASSOCIATED CONTENT

Supporting Information. Additional information including three figures and three tables. This material is available free of charge via the Internet at http://pubs.acs.org.

■ AUTHOR INFORMATION

Corresponding Author
*E-mail: yzhang9@uwyo.edu.

■ ACKNOWLEDGMENT

Acknowledgment is made to the donors of the American Chemical Society Petroleum Research Fund (ACS PRF Grant No. 48773-DNI 8) for partial support of this research. Support from the National Science Foundation (EAR-0838250) is acknowledged, as well as the School of Energy Resources at the University of Wyoming through its Matching Grant Fund Program. We thank Schlumberger Information Solutions for software donation and technical support.

■ REFERENCES

(1) IPCC. Carbon Dioxide Capture and Storage, Chp 5, Underground Geological Storage. http://www.ipcc.ch/pdf/special-reports/srccs/ (accessed July 24, 2007).

(2) Gerritsen, M.; Durlofsky, L. J. Modeling fluid flow in oil reservoirs. *Annu. Rev. Fluid Mech.* **2005**, 211−238, doi: 10.1146/annurev.fluid.37.061903.175748.

(3) Friedmann, F.; Chawathe, A.; Larue, D. Assessing uncertainty in channelized reservoirs using experimental designs. *SPE*, **2003**, Paper Number 85117.

(4) Narahara, G.; Spokes, J.; Brennan, D.; Maxwell, G.; Bast, M. *Well Count Optimization Incorporating a Wide Range of Uncertainties for the Deepwater Agbami Field*, 16988. ; *SPE*: Houston, TX, May 3—6, 2004.

(5) Bryant, S.; Lakeshminarasimhan, S.; Pope, G. A. Buoyancy-dominated multiphase flow and its effect on geological sequestration of CO_2. *SPE J.* **2008**, 447–454.

(6) Zhang, Y.; Liu, B.; Gable, C. W. Homogenization of hydraulic conductivity for hierarchical sedimentary deposits at multiple scales. *Transp. Porous Media* **2011**, DOI: 10.1007/s11242-010-9711-8.

(7) Eccles, J. K.; N., R. G.; Pratson, L.; Jackson, R. B. Phyisical and economic potential of geologic CO_2 storage in saline aquifers. *Envrion. Sci. Technol.* **2009**, *43*, 1962–1969.

(8) Doughty, C.; Pruess, K. Modeling supercritical carbon dioxide injection in heterogeneous porous media. *Vadose Zone J.* **2004**, *3*, 837–847.

(9) Montgomery, D. C. *Design and Analysis of Experiments*, 7th ed.; John Wiley & Sons, Inc: New York, 2008.

(10) Milliken, W.; Levy, M.; Strebelle, S.; Zhang, Y. The effect of geologic parameters and uncertainties on subsurface flow: Deepwater depositional systems. *SPE*, **2007**, Paper Number 109950.

(11) Myers, R.; Montgomery, D. *Response Surface Methodology—Process and Product Optimization Using Designed Experiments*; John Wiley & Sons: New York, 1995.

(12) Michael, K.; Golab, A.; Shulakova, V.; Ennis-King, J.; Allinson, G.; Sharma, S.; Aikeen, T. Geological storage of CO_2 in saline aquifers—A review of the experience from existing storage operations. *Int. J. Greenhouse Gas Control* **2010**, *4*, 659–667.

Supporting Information Available

4 SUPPLEMENTAL

4.1 Numerical Simulation of CO_2 Injection

CO_2 injection is simulated with GASWAT (2009), a multiphase compositional simulator applicable to modeling CO_2 flow in deep saline aquifers (*13*). Two phases are considered: a CO_2-rich supercritical phase (or "gas" phase) and a H_2O-rich liquid phase. CO_2 density is computed based on a cubic equation of state tuned to experimental measurements, while liquid density is corrected for total dissolved solids (salinity). Between the two phases, two components (CO_2, H_2O) are modeled; each component can exist in both phases. The simulator first solves the pressure and molar density of each component. The mole fractions of the components in the phases are then computed through a flash process, where mutual solubilities of CO_2 and H_2O are calculated to match experimental data. A modified Peng-Robinson Equation of State is used to calculate gas solubility in the aqueous phase when water salinity is high.

A constant reservoir temperature is specified, based on model depth, geothermal gradient, and a fixed surface temperature. GASWAT does not solve the heat balance equation, thus the reservoir temperature is not perturbed by CO_2 flow (temperature is used to compute the in-situ fluid properties). The storage model is saturated with brine prior to CO_2 injection. Water is assumed to be the wetting phase, CO_2 the non-wetting phase. Rock compressibility is assigned using a typical value for sandstones. Relative permeability functions are based on experimental measurements (see 5.2 for details). To model flow reversal in a grid cell before the maximum gas saturation is reached, the Carlson method is used for scanning curve interpolation between the bounding relative permeability curves (*14*).

The storage model is assumed to be part of a larger regional flow system, thus open boundary (constant-head) is assigned to the model sides, which allows both gas and brine to migrate laterally out of the aquifer. This boundary condition also prevents pressure buildup in the model. The

injector bottomhole pressure (BHP) is checked against a fracture pressure, which is evaluated at the model depth as 1.6 $\times$ hydrostatic pressure (the piezometric head of the aquifer is assumed to be at the land surface). In all simulations of the SA, by setting the fracture pressure as the BHP constraint for the injector, the fracture pressure is never exceeded.

4.2 Input Variables

The SA for each storage model varies a select set of input parameters, while keeping others constant. The constant parameters are those that either do not vary (e.g., gravitational constant), or their variations are typically small at a storage site (e.g., porosity, rock/fluid compressibility). The parameters that are varied in the SA are those that can exhibit large uncertainties at a storage site. All model parameters are listed in Table 1, including their values used by simulations or ranges varied in the SA. For the parameters varied in the SA, detailed justifications are provided below.

Table 1: **Model parameters and their values. Parameters varied in the SA are labeled as "variable".**

Parameter	Symbol	Value	Unit	Note
porosity (caprock)	ϕ	0.01		fixed
porosity (aquifer)	ϕ	0.15		fixed
irreducible water saturation	S_{wi}	0.42		fixed
gas endpoint relative permeability	k_{rg}^{end}	0.26		fixed
water endpoint relative permeability	k_{rw}^{end}	1.0		fixed
drainage connate water saturation	S_w^d	0.06		fixed
critical gas saturation	S_g^{cr}	0.06		fixed
temperature (land surface)	T	15	^{o}C	fixed
hydrostatic pressure gradient	∇P	0.10	bar/m	fixed
rock compressibility	β	1.4×10^{-5}	1/bar	fixed
depth of the top of the grid	D	1000–3000	m	variable
residual gas saturation	S_g^r or SGR	0.06–0.42		variable
salinity	SAL	10,000–260,000	ppm	variable
injection rate	q	0.45–0.90	kg/s	variable
regional (vertical) hydraulic gradient	AquG	-0.03–0.03	m/m	variable
caprock permeability	krock	10^{-8}–10^{-4}	mD	variable
geothermal gradient	TG	0.025-0.050	^{o}C/m	variable
aquifer lnk variance	VAR	0.1–7.0	mD^2	variable

(1) Gradient of the background aquifer flow (AquG). In sedimentary basins, background flow can exist when the storage aquifer is part of a larger groundwater system. A vertical background

flow can potentially impact storage security: downward moving groundwater may deter upward migration of the injected CO_2; upward moving groundwater may enhance upward gas flow and residual gas trapping during imbibition. Two end-member conditions are assumed by assigning a +/-3% hydraulic head gradient to AquG across the vertical extent of the model. The value of AquG affects the initial condition in CO_2 simulation. When AquG is non-zero, upward or downward flow of groundwater is simulated first in the storage system until steady-state is reached at the specified gradient. The pressure of this dynamic flow field then provides the initial condition for CO_2 simulation. In the pre-simulation, when AquG is 3% (upward flow), two external aquifers are linked to the top and bottom of the storage model, each equilibrated with a different hydraulic potential. The potential difference then drives flow. When AquG is -3% (downward flow), a single external aquifer is linked to the top of the storage model, while the bottom of the model is no-flow. When AquG is at the mid value of 0.0, there is no vertical background flow (same potential is assigned to the external aquifers). In this case, since the lateral groundwater gradient is always 0.0, the initial condition for CO_2 simulation is hydrostatic. During CO_2 simulation, the same external aquifers used to establish the initial condition are linked to the storage model, driving background flow (or no flow) concurrent with the CO_2 operation.

(2) Geothermal gradient (TG). Temperature in the storage model can affect density of the injected CO_2. Colder basins are considered more favorable than warmer basins, since cooler temperature reduces CO_2 buoyancy and more CO_2 mass can be stored per unit pore volume in the aquifer (*15*). Temperature of a storage system depends on factors such as geothermal gradient, depth, and surface temperature. In the present study, a fixed surface temperature is assumed. A geothermal gradient is chosen to vary between 25 and 50 ^oC/km (*15*).

(3) Strength of aquifer heterogeneity (VAR). Though past research has investigated the influence of heterogeneity on CO_2 flow (*16*, *17*), the present study explores questions such as: is geological heterogeneity favorable to CO_2 storage? Can simple models be used to make predictions, ignoring underlying heterogeneity? And, is the adequacy of the simple models affected by the strength of heterogeneity? VAR is aquifer lnk variance of the FHM, which is scaled to 3 values

in the SA: 0.1, 1.0, and 7.0, representing a weakly to strongly heterogeneous system (*18*). During this scaling, the mean lnk of the aquifer remains fixed, thus only the spread of the heterogeneity is affected. As a result, three sets of permeability data are created for the FHM, based on which three sets of equivalent permeabilities are computed for the units of the stratigraphic models.

(4) Gas phase relative permeability hysteresis (SGR). The importance of residual gas trapping due to non-wetting phase relative permeability hysteresis is widely recognized, though uncertainty exists in the magnitude of this hysteresis for the CO_2/brine system. In this study, a uniform set of relative permeability functions is assigned to the aquifer, though residual gas saturation is varied between 0.06 to 0.42, representing zero to large gas phase relative permeability hysteresis (Figure 1). These functions are constructed using experimental data for the Viking Sandstone (*19*). For the caprock, a separate set of non-hysteretic relative permeability functions is used based on those measured for the low-permeability Calmar Formation in the Alberta Basin (*20*).

(5) Salinity (SAL). Salinity affects CO_2 dissolution in brine (*21*) as well as brine density. Salinity is varied from 10,000 to 260,000 ppm. 10,000 ppm is the lower limit at which a deep aquifer qualifies for CO_2 storage; 260,000 ppm is the upper limit of applicability for the solubility module of GASWAT.

(6) Injection rate (q). Injection rate can affect the lateral extent of the injected CO_2. Increasing rate increases the viscous driving force which enhances lateral spreading, thus more trapping and dissolution. Higher rate can also create higher local pressure gradient near the injector, which leads to higher maximum gas saturation before flow reversal. Following the scanning curve that is closer to the bounding imbibition curve, the higher gas saturation will lead to more residual trapping during imbibition. The injection rate is varied between 0.45 and 0.9 kg/s, the later being the largest rate at which convergence issues will not occur in all the simulation runs, while satisfying the BHP constraint. Note that when higher rates were initially attempted, some DoE runs could not converge after a long simulation time (e.g., 3 weeks). The injection rate used here reflects a pilot-scale scenario, which is not fully realistic considering that commercial-scale injection rate can be higher. Future work will consider larger rates after the simulator issues and constraints are first

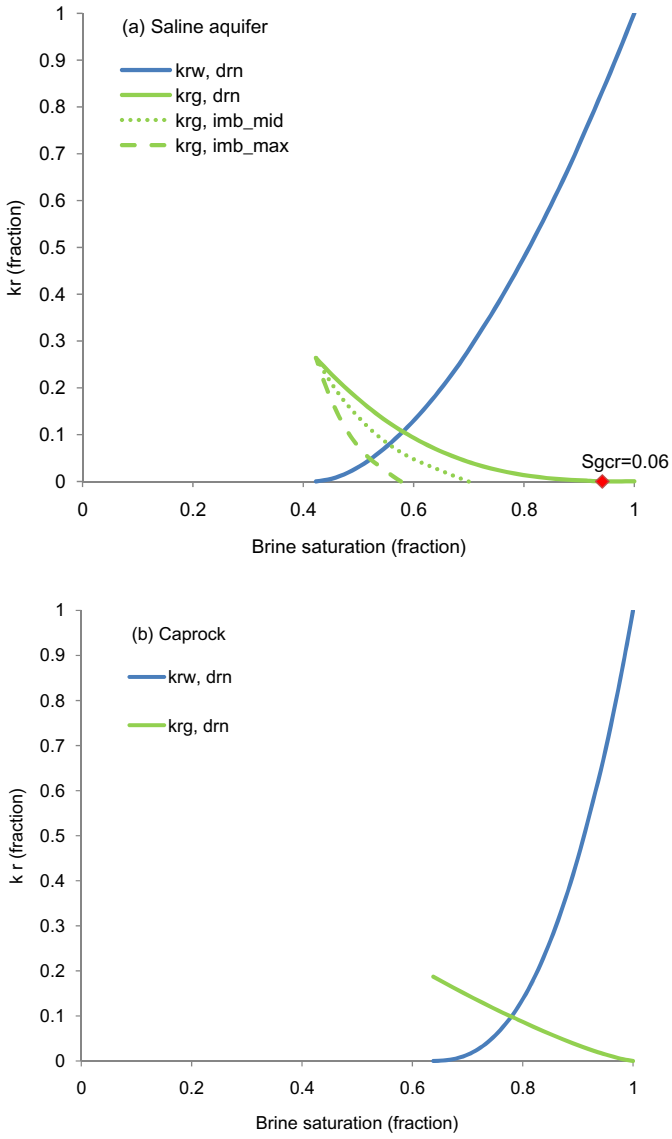

Figure 1: **Relative permeability functions for the aquifer (a) and the caprock (b). In the SA, the residual gas saturation (SGR) in the aquifer is varied, i.e., the 3 bounding imbibition curves in (a), one coinciding with the drainage curve when SGR is 0.06 (Table 1). In this case, SGR = S_g^{cr} (critical gas saturation) and gas phase relative permeability is non-hysteretic.**

overcome.

(7) Caprock permeability (krock). Caprock permeability can influence not only gas and brine migration but also the evolution of reservoir fluid pressure, particularly if the formation is compartmentalized (not considered here) (*22*). A set of preliminary simulations was conducted first to identify a maximum krock of $1x10^{-4}$ mD without leading to significant gas-phase leakage. In these simulations, all other parameters assumed their center values, thus the maximum krock found is not necessarily applicable to all parameter combinations. krock is assumed to vary between $1x10^{-4}$ and $1x10^{-8}$ mD, based on values observed for shale and clay-rich rocks.

4.3 Results at 1 km & 3 km Depths

The SA is repeated for all models, with the system depth adjusted to 1 and 3 km, respectively. Important parameters to the same set of prediction outcomes are compiled (Table 2, Table 3). Compared to the results at 2 km (Table 3), the most significant difference occurs at 3 km, during early monitoring: TG becomes important to predicting brine leakage (positive effect), dissolved gas (positive effect), and mobile gas (negative effect). This suggests that within the parameter space, the importance of geothermal gradient to predictions is affected by changing depth, though such effects are mostly secondary.

Table 2: **Results of SA at 1 km depth.**

Outcomes	**Models**	**End of Injection**	**Monitoring Period (Years After Injection Ends)**				
			100	200	300	400	500
Trapped Gas	FHM	SGR	SGR/VAR/SAL	SGR/VAR/SAL	SGR/SAL/VAR	SGR/SAL/VAR	SGR/SAL/VAR
	8UNIT	VAR/SGR	SGR/VAR/SAL/AquG	SGR/VAR/SAL	SGR/VAR/SAL	SGR/VAR/SAL	SGR/VAR/SAL
	3UNIT	SAL/TG/VAR/q	SAL/VAR/TG	SAL/VAR/TG/SGR	SAL/VAR/TG/SGR	SAL/VAR/TG/SGR	SAL/VAR/TG/SGR
	1UNIT	SGR/SAL/q	SGR	SGR	SGR/SAL	SGR/SAL	SGR/SAL/VAR
Dissolved Gas	FHM	SAL/VAR/TG	SAL/VAR	SAL/VAR/SGR	SAL/VAR/SGR	SAL/VAR/SGR	SAL/VAR/SGR
	8UNIT	SAL/TG/VAR/q	SAL/VAR/TG	SAL/VAR/TG/SGR	SAL/VAR/TG/SGR	SAL/VAR/TG/SGR	SAL/VAR/SGR/TG
	3UNIT	SAL/TG/VAR/q	SAL/VAR/SGR/TG	SAL/VAR/SGR/TG	SAL/VAR/SGR/TG	SAL/VAR/SGR/TG	SAL/SGR/VAR
	1UNIT	SAL/TG	SAL/SGR/TG/VAR	SAL/SGR/TG/VAR	SAL/SGR/TG/VAR	SAL	SAL/SGR/TG
Mobile Gas	FHM	VAR	SGR/VAR	SGR/VAR	SGR/VAR	SGR/VAR/SAL	SGR/VAR/SAL
	8UNIT	VAR/SAL/TG/SGR	SGR/VAR/AquG/SAL/TG	SGR/VAR/SAL	SGR/VAR/SAL	SGR/VAR/SAL	SGR/VAR/SAL
	3UNIT	VAR/SAL	SGR/VAR/AquG/SAL/TG	SGR/VAR/SAL/AquG/TG	SGR/VAR/SAL	SGR/VAR/SAL	SGR/VAR/SAL
	1UNIT	SAL/q/SGR/AquG	SGR/VAR	SGR	SGR	SGR	SGR/VAR
Brine Leakage	FHM	krock	krock/AquG/TG	krock/AquG	krock/AquG	krock/AquG	krock/AquG
	8-UNIT	krock	krock/AquG/TG	krock/AquG	krock/AquG	krock/AquG	krock/AquG
	3-UNIT	krock	krock/AquG/TG	krock/AquG	krock/AquG	krock/AquG	krock/AquG
	1-UNIT	krock	krock/AquG/TG	krock/AquG	krock/AquG	krock/AquG	krock/AquG

Table 3: **Results of SA at 3 km depth.**

Outcomes	Models	End of Injection	Monitoring Period (Years After Injection Ends)				
			100	200	300	400	500
Trapped Gas	FHM	SGR/VAR	SGR/SAL/VAR	SGR/SAL/VAR	SGR/SAL/VAR	SGR/SAL/VAR	SGR/SAL/VAR
	8UNIT	SGR	SGR/SAL/VAR	SGR/VAR/SAL	SGR/VAR/SAL	SGR/SAL/VAR	SGR/SAL/VAR
	3UNIT	SGR	SGR/SAL	SGR/SAL/VAR	SGR/SAL/VAR	SGR/SAL/VAR	SGR/SAL/VAR
	1UNIT	SGR/SAL	SGR/SAL	SGR/SAL	SGR/SAL	SGR/SAL	SGR/SAL
Dissolved Gas	FHM	SAL/TG/VAR	SAL/VAR/TG/SGR	SAL/VAR/SGR/TG	SAL/VAR/SGR/TG	SAL/VAR/SGR/TG	SAL/VAR/SGR/TG/krock
	8UNIT	SAL/TG/VAR/q	SAL/TG/VAR	SAL/VAR/TG	SAL/VAR/TG	SAL/VAR/TG	SALVAR/TG/SGR
	3UNIT	SAL/TG/VAR/q	SAL/TG/VAR	SAL/TG/VAR	SAL/TG/VAR	SAL/VAR/TG/SGR	SAL/VAR/TG/SGR
	1UNIT	SAL/TG	SAL/TG/SGR	SAL/TG/SGR	SAL/TG/SGR/VAR	SAL/TG/SGR/VAR	SAL/TG/SGR/VAR
Mobile Gas	FHM	VAR	SGR/VAR/TG/krock	SGR/VAR/TG	SGR/VAR	SGR/VAR	SGR/VAR
	8UNIT	SAL/VAR/TG	SGR/VAR/TG/AquG	SGR/VAR/TG	SGR/VAR/TG	SGR/VAR/TG/SAL	SGR/VAR/SAL
	3UNIT	SAL	SGR/VAR/TG/AquG	SGR/VAR/TG	SGR/VAR/TG	SGR/VAR	SGR/VAR
	1UNIT	SAL/SGR/q	SGR/TG	SGR/TG/q/VAR	SGR/TG	SGR	SGR
Brine Leakage	FHM	krock	krock	krock/AquG/TG	krock/AquG/TG	krock/AquG/TG	krock/AquG
	8-UNIT	krock	krock/AquG/TG	krock/AquG/TG	krock/AquG/TG	krock/AquG	krock/AquG
	3-UNIT	krock	krock/AquG/TG	krock/AquG/TG	krock/AquG	krock/AquG	krock/AquG
	1-UNIT	krock	krock/AquG/TG	krock/AquG/TG	krock/AquG	krock/AquG	krock/AquG

4.4 Gas Profile and Plume Shape Predictions

Since VAR is consistently identified as an important parameter impacting gas predictions, three runs with low (Run 1), intermediate (Run 7), and high (Run 6) VAR are presented. The model depth is 2 km. In each run, performance of the stratigraphic models is compared with that of the FHM.

Gas profiles are compared first (Figure 2): (1) in all runs, the 8-Unit model is the most accurate, followed by the 3-Unit and 1-Unit models. (2) when variance is low, prediction errors of the stratigraphic models are smaller, vice versa.

Gas plumes simulated by the same models are visualized next (Figure 3). Here, only the plumes simulated by the low-variance Run 1 and high-variance Run 6 are shown. For the Run 1 simulations, all models predict very similar plume shapes, at both time scales (end of injection, end of monitoring). This suggests that when the system variance is low, an optimal stratigraphic model for predicting the plume shape is the 1-unit model.

When variance is higher, the FHM predicts a plume that is more laterally spread out. During injection, a sub plume develops in this model through a high permeability pathway, as discussed in the article. At the end of injection, a small amount of gas has reached and pooled beneath the caprock. During the monitoring phase, this gas cap expands slowly, while the overall plume shape does not change significantly. In contrast to Run 1, plume shapes predicted by the stratigraphic

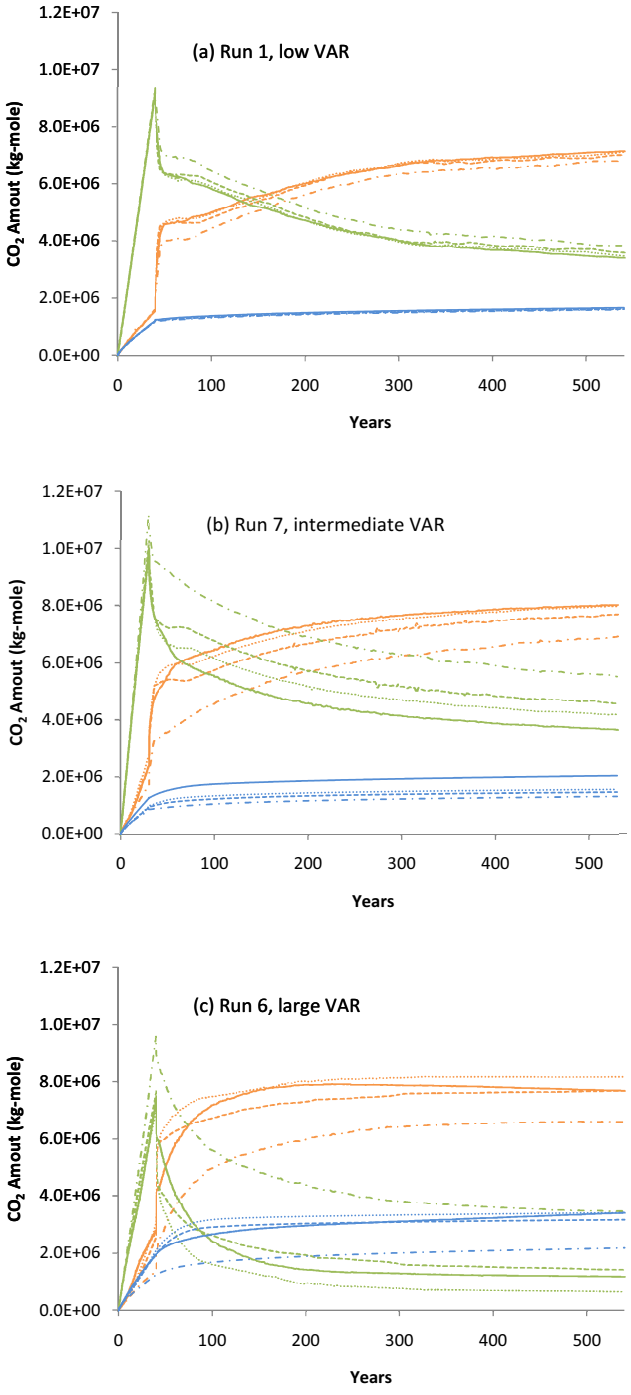

Figure 2: **Trapped (orange), mobile (green), and dissolved (blue) CO_2 over time, at low (a), intermediate (b), and large (c) aquifer lnk variances. All model predictions are shown: FHM (solid), 8-Unit (dotted), 3-Unit (dashed), and 1-Unit (dash-dot).**

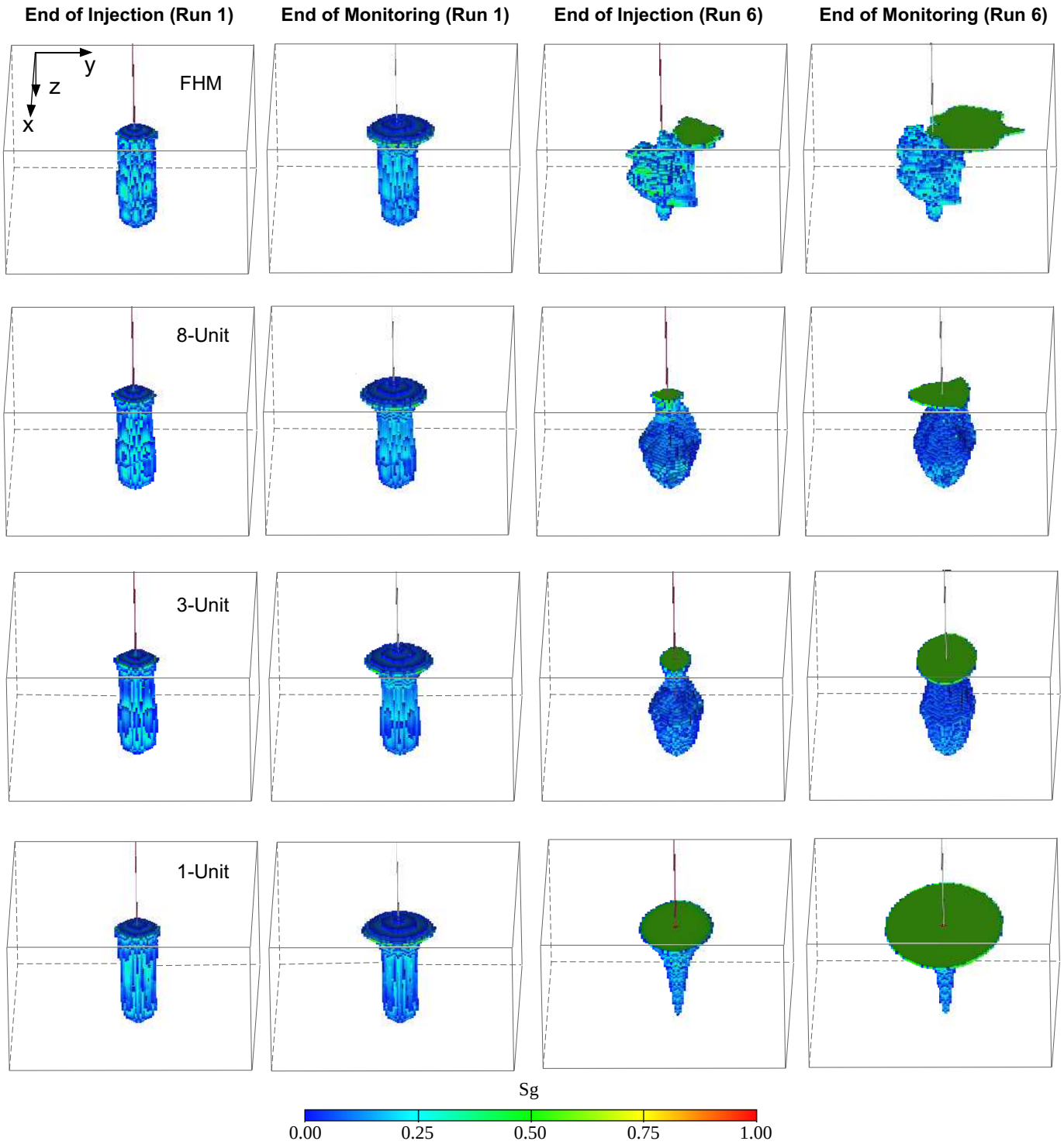

Figure 3: **Gas plume visualization at the end of injection and monitoring. S_g includes both mobile and trapped gas. Depth = 2km. Run 1 is of low variance; Run 6 is of high variance. First row: FHM; Second row: 8-unit model; Third row: 3-unit model; Fourth row: 1-unit model. Box indicates model boundary including the caprock unit.**

models deviate significantly from those of the FHM, in particular, the sub plume is not predicted by these models. The 1-unit model is the worst predictor which gives the classic plume shapes of a homogeneous formation. Comparing the 8-unit and 3-unit models, however, their predictions only differ slightly, consistent with their mass profile results (Figure 2). When the system variance is higher, an optimal stratigraphic model for predicting the plume shape is the 3-unit model.

This material is available free of charge via the Internet at `http://pubs.acs.org/`.

References

(1) IPCC, Carbon Dioxide Capture and Storage, Chp 5, Underground Geological Storage. http://www.ipcc.ch/pdf/special-reports/srccs/.

(2) Gerritsen, M.; Durlofsky, L. J. Modeling Fluid Flow in Oil Reservoirs. *Annual Review of Fluid Mechanics* **2005**, 211–238, doi: 10.1146/annurev.fluid.37.061903.175748.

(3) Friedmann, F.; Chawathe, A.; Larue, D. Assessing Uncertainty in Channelized Reservoirs using Experimental Designs. *SPE,* **2003**, Paper Number 85117.

(4) Narahara, G.; Spokes, J.; Brennan, D.; Maxwell, G.; Bast, M. Well count optimization incorporating a wide range of uncertainties for the deepwater Agbami Field. 2004; SPE 16988, Houston, Texas, U.S.A., May 3—6, 2004.

(5) Bryant, S.; Lakeshminarasimhan, S.; Pope, G. A. Buoyancy-Dominated Multiphase Flow and its Effect on Geological Sequestration of CO_2. *SPE Journal,* **2008**, 447–454.

(6) Zhang, Y.; Liu, B.; Gable, C. W. Homogenization of Hydraulic Conductivity for Hierarchical Sedimentary Deposits at Multiple Scales. *Transport in Porous Media,* **2011**, *Accepted for Publication*.

(7) Jordan K. Eccles, R. G. N., Lincoln Pratson; Jackson, R. B. Phyisical and Economic Potential of Geologic CO2 Storage in Saline Aquifers. *Envrionmental Science and Technology,* **2009**, *43*, 1962–1969.

(8) Doughty, C.; Pruess, K. Modeling Supercritical Carbon Dioxide Injection in Heterogeneous Porous Media. *Vadose Zone Journal,* **2004**, *3*, 837–847.

(9) Montgomery, D. C. *Design and Analysis of Experiments*, 7th ed.; John Wiley & Sons, Inc, 2008.

(10) Milliken, W.; Levy, M.; Strebelle, S.; Zhang, Y. The Effect of Geologic Parameters and Uncertainties on Subsurface Flow: Deepwater Depositional Systems. *SPE,* **2007**, Paper Number 109950.

(11) Myers, R.; Montgomery, D. *Response Surface Methodology — Process and Product Optimization Using Designed Experiments*; John Wiley & Sons: New York, 1995.

(12) Michael, K.; Golab, A.; Shulakova, V.; Ennis-King, J.; Allinson, G.; Sharma, S.; Aikeen, T. Geological storage of CO2 in saline aquifers - a review of the experience from existing storage operations. *International Journal of Greenhouse Gas Control* **2010**, *4*, 659–667.

(13) Schlumberger, ECLIPSE Technical Manual: the GASWAT Option. 2009.

(14) Carlson, F. Simulation of relative pearmeability hysteresis to the non-wetting phase. *SPE,* **1981**, 1962–1969, Paper Number 10157.

(15) Bachu, S. Screening and Ranking of Sedimentary Basins for Sequestration of CO_2 in Geological Media in Response to Climate Change. *Environmental Geology,* **2003**, *44*, 277–289.

(16) Ashraf, M.; Lie, K.-A.; Nilsen, H. M.; Nordbotten, J. M.; Skorstad, A. Impact of Geological Heterogeneity on Early-Stage CO_2 Plume Migration. 2010; XVIII International Conference on Water Resources, June 2010, Barcelona.

(17) Oloruntobi, O. S.; LaForce, T. Effect of Aquifer Heterogeneity on CO_2 Sequestration. *SPE,* **2009**, Paper Number 121776.

(18) Gelhar, L. W. *Stochastic Subsurface Hydrology*; Prentice Hall College Div, 1993.

(19) Bennion, D. B.; Bachu, S. Drainage and Imbibition Relative Permeability Relationships for Supercritical CO_2/Brine and H_2S/Brine Systems in Intergranular Sandstone, Carbonate, Shale, and Anhydrite Rocks. *SPE,* **2008**, Paper Number 99326.

(20) Bennion, D. B.; Bachu, S. Permeability and Relative Permeability Measurements at Reservoir Conditions for CO_2-Water Systems in Ultra Low Permeability Confining Caprocks. *SPE,* **2007**, Paper Number 106995.

(21) Chang, Y.; Coats, B. K.; Nolen, J. S. A Compositional Model for CO_2 Floods Including CO_2 Solubility into Water. *SPE Reservoir Evaluation and Engineering* **1998**, *1*, 155–160.

(22) Birkholzer, J.; Zhou, Q.; Tsang, C.-F. Large-scale impact of CO2 storage in deep saline aquifers: A sensitivity study on pressure response in stratified systems. *International Journal of Greenhouse Gas Control* **2009**, *3*, 181–194.